L30

EXPLOITATION OF X-RAY DIFFRACTION IN CHARACTERISATION OF C45 FERRITIC-PEARLITIC STEEL PROPERTIES

D. Šimek[1], A. Oswald[2], R. Schmidtchen[2], M. Motylenko[1], D. Rafaja[1], G. Lehmann[2]

[1]*Institute of Materials Science, TU-Freiberg, Gustav-Zeuner-Str. 5, D-09599 Freiberg, Germany*
[2]*Institute of Metal Forming, TU-Freiberg, Bernhard von Cotta Str. 4, D-09599 Freiberg, Germany*
e-mail: simek@fzu.cz

Ferritic-pearlitic (F-P) steel C45 containing 0.45 wt.% of carbon exhibits a variable microstructure according to its thermo-mechanical treatment. After forming in austenite state, if the cooling below approx. 850 °C is slow enough, the ferritic-pearlitic microstructure develops. The primary ferrite crystallizes at the austenitic grain boundaries above the eutectoid temperature of 727 °C, below which the rest austenite is transformed into lamellar pearlite. The relative amount of primary ferrite (X_f) depends on the cooling rate, the prior austenite grain size (the smaller the grains the larger the grain boundary crystallisation area) and the upper limit is approx. 60%. The faster the cooling, the less primary ferrite is developed in favour of pearlite.

The correlation of mechanical properties of F-P steels wit their microstructure were thoroughly studied [1,2,3] as the key factors affecting the strength of pearlite, its interlamellar distance (ILD, S) was identified [1,2]. In F-P steels, the volume fraction of pearlite ($X_p = 1 - X_f$) play also an important role, but the correlation of yield strength with these two parameters is not clear [3].

The intention of study was to investigate the exposure of the microstructure in the X-ray diffraction (XRD) and the correlation of XRD features with mechanical properties of C45 F-P steel directly. The aim of the survey was to develop a fast analytical method for an on-line control of manufacturing process optimisation. In order to cope with the problem, a series of F-P microstructures was produced by hot rolling at various temperatures and by different regimes of cooling (ambient air, lead bath of 550 °C, dipping in water). Subsequent heating was optionally also applied. Further, selected F-P microstructures representing the broad range of hot rolled F-P steels were subjected to gradual cold drawing with or without intermediate reheating. This process represented the industrial treatment from ingots till cold-drawn hard wires.

The investigation of the hot rolled samples revealed that the ferrite phase is under an apparent compressive residual stress regardless of the cut of the specimen surface (cross-sectional or longitudinal). This behaviour excludes the macroscopic residual stress. It is a consequence of two-component microstructure (ferrite/pearlite). The TEM investigation revealed the misfit dislocations at the ferrite cementite interfaces in the pearlite, while the primary ferrite grains were almost defect-free. The 3rd kind dislocation induced mean squared microstrain (ε^2_{disl}) obtained from XRD was found to correlate with the over-all density of cementite lamellas calculated as X_p/S (Figure 1). The same tendency is held also for fully pearlitic samples of steel C80D (0.80 wt.% carbon). The dependence is rather quadratic instead of linear as supposed in e.g. [4]. It is the nature of the misfit dislocations that are not randomly distributed but organized in an equidistant grid, so that their displacement fields are more similar to dislocation dipoles. The ultimate tensile strength was found to be directly proportional to the mean squared microstrain in hot-rolled samples (Figure 2).

With cold drawing, for cross-sectional reduction till about 50%, the dislocation density increases and the correlation of UTS with the mean squared microstrain can still

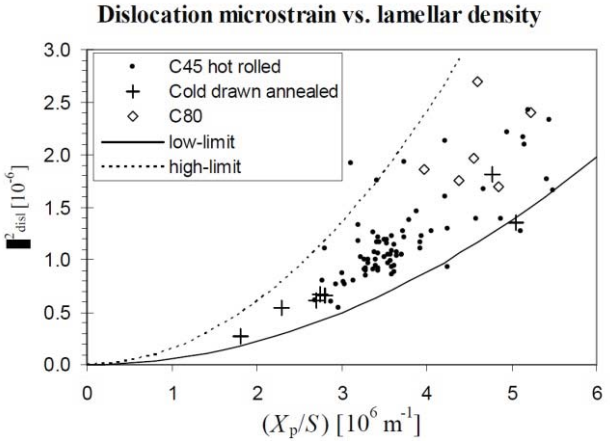

Figure 1. Correlation of dislocation-induced microstrain and over-all lamellar density in hot rolled ferritic-pearlitic C45 samples and in fully pearlitic (C80) samples. The cold drawn and subsequently annealed C45 samples are also included.

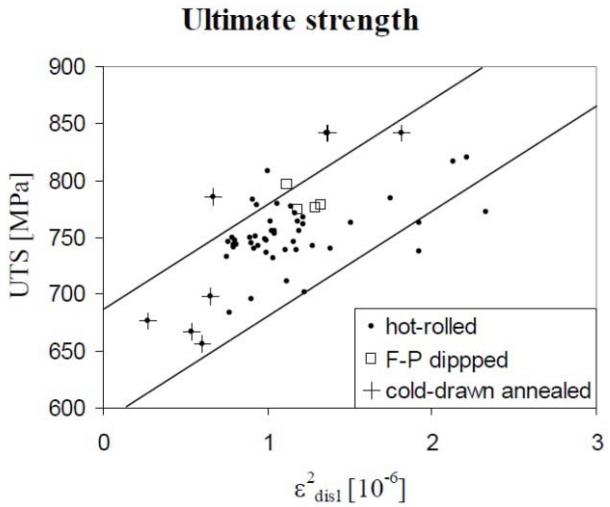

Figure 2. Correlation of UTS with mean squared dislocation induced microstrain.

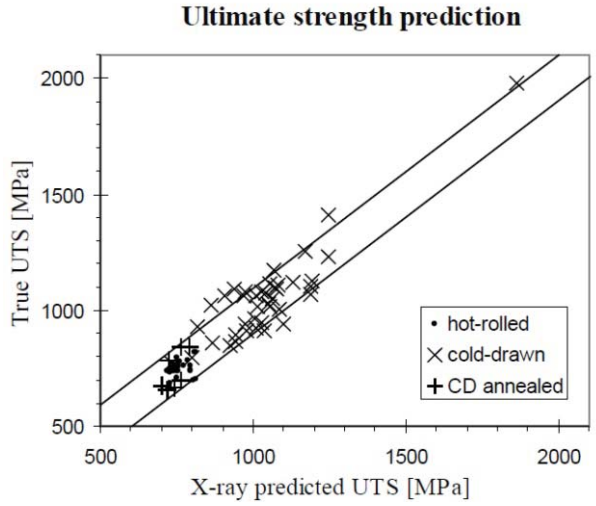

Figure 3. Comparison of UTS predicted from the X-ray diffraction experiment and true UTS evaluated in the tensile test

be observed, however, with a certain offset in the microstrain compared to hot rolled samples. Afterwards, for higher deformation or after annealing, the proportionality is lost. On the other hand, macroscopic residual stress is now observed in the ferrite phase, which is compressive along drawing direction. It is the result of the easier plastic deformation of the ferrite compared to harder cementite, which, after relief of the drawing force, compresses the ferrite.

A new empirical correlation was found between the UTS and the (extrapolated) lattice parameter observed on crystallographic direction ⟨111⟩ in the drawing direction (a_{111}). The smaller is the a_{111} (the stronger the compressive force), the higher is the UTS of the steel in the tensile test. The XRD here allows to determine which mechanism is driving the tensile properties. Thus, a single measurement in rolling/drawing direction is suitable for estimation of the UTS. If the a_{111} is larger than the stress-free lattice parameter, the sample is hot rolled or annealed and UTS depends on the dislocation density (analysed from the line broadening). If a_{111} is smaller, the UTS is dependent upon this lattice parameter. The XRD-predicted UTS than gives a good agreement with the true experimental UTS evaluated from the tensile test (Figure 3).

The XRD is able to predict the ultimate tensile strength of ferritic-pearlitic steel produced by the hot rolling or cold drawing in a broad range of its experimental values (600 – 2000 MPa) with the error band of approx. ± 100 MPa (cf. Figure 3). It appears therefore as a promising analytical method for a fast on-line control of the steel production. The correlation with the microstructure moreover allows to estimate the mesoscopic microstructure parameter (pearlite volume fraction or its interlamellar distance) if additional information about the thermo-mechanical history is known.

1. O. P. Modi, N. Deshmukh, D. P. Mondal, A. K. Jha, A. H. Yegneswaran, H. K. Khaira, *Materials Characterization* **46**, (2001), pp. 347-352.
2. A. M. Elwazri, P. Wanjara, S. Yue, *Mat. Sci. Eng. A* **404**, (2005), pp. 91-98.
3. K. K. Ray, D. Mondal, *Acta Metall. Mater.* **39**, (1991), pp. 2201-2208.
4. T. Ungár, I. Dragomir, Á Révész, A. Borbély, *J. Appl. Cryst.* **32**, (1999), pp. 992-1002.

L31

TOWARD THE FINAL EXPLANATION OF MARTENSITIC TRANSFORMATION IN SHAPE MEMORY ALLOY CO-NI-AL

J. Kopeček[1], M. Jarošová[2], K. Jurek[2], J. Drahokoupil[1], I. Kratochvílová[1], L. Fekete[1], L. Bodnárová[3], H. Seiner[3], P. Sedlák[3], M. Landa[3], J. Šepitka[4], J. Lukeš[4], V. Kopecký[1], O. Heczko[1]

[1] Institute of Physics of the AS CR, Na Slovance 2, 182 21 Praha 8, Czech Republic
[2] Institute of Physics of the AS CR, Cukrovarnická 10/112, 162 00 Praha 6, Czech Republic
[3] Institute of Thermomechanics of AS CR, Dolejškova 5, 182 00 Prague 8, Czech Republic
[4] Laboratory of Biomechanics, CTU in Prague, Technická 4, 166 07, Prague 6, Czech Republic
kopecek@fzu.cz

Great success in Ni_2MnGa derived alloys [1,2] attracted attention to similar Heusler alloys including cobalt based CoNiAl and CoNiGa [3,4]. As the NiMnGa alloys suffer due to their strongly intermetallic state (brittleness, poor creep and fatigue properties) the cobalt based alloys seemed to be the interesting candidate for the mechanically stronger and more resistant FSMAs.

The article describes the progress in work on $Co_{38}Ni_{33}Al_{29}$ alloy [5,6]. The defined crystals with single-crystalline matrix were prepared after long struggling. The influence of annealing on martensitic transformation was investigated. Both post-mortem XRD and in-situ neuron diffraction confirmed the martensitic phase transformation of alloy matrix B2 ↔ $L1_0$ and stable amount of A1 particles (fcc cobalt solid solution) in alloy, Fig. 1. The image of transformation paths is blurred considering the results of resonant ultrasound spectroscopy (RUS), magnetic susceptibility measurements and various microscopies (LOM, SEM, AFM), which shows transformation temperature significantly higher (about approx. 70 °C). Without regard to structural confusion all samples perform

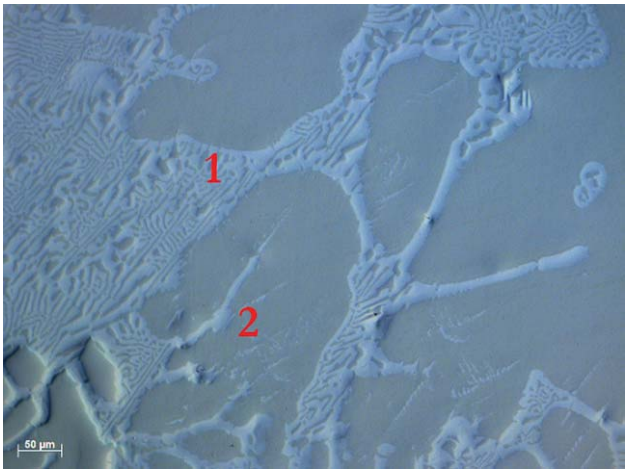

Figure 1. The structure of the samples observed by scanning electron microscopy. The precipitates marked 1 are interdendritic A1 fcc cobalt solid solution particles. The precipitates marked 2 are $L1_2$ ordered precipitates of the phase $(Co,Ni)_3Al$.

pseudoelastic behaviour at room temperature, which is strongly dependent on crystallographic orientation.

Nevertheless, the role of nanoprecipitates resulting from segregation in oversaturated matrix after annealing or other changes in matrix induced by quenching seems to be indisputable [7]. These precipitates can serve as nucleation centres for the stress induced martensitic transformation. Nanoprecipitates were observed in annealed samples but in both pseudoelastic [8] and non-pseudoelastic samples [9]. The wide variety of nanoprecipitates is described in Ref. [4], nevertheless their necessity for pseudoelastic behaviour was not proven. The many micron-sized non-twinned, single and triple $\{111\}_p$ twinned precipitates with partial $L1_2$ ordering were observed in the austenite matrix after annealing at 1373 K for 72 h and quenching [10]. The final description of A1 interdendritic particles dissolution and the role of precipitation after quenching is still under the process.

The more optimistic view we have now on various results of "transformation" given by different methods. The strong magnetoelastic coupling can be documented by the evolution of damping in RUS [11]. Surprisingly the effect of magnetic field in Co-Ni-Al austenite, considering the external field, is very weak [12]. We can expect now that the finalization of the oriented cuboid samples will give us the full elastic constants set in temperature dependence and the story of "martensitic transformation" in Co-Ni-Al alloys would be finally explained.

1. Heczko O., Scheerbaum N., Gutfleisch O., *Magnetic Shape Memory Phenomena*, in *Nanoscale Magnetic Materials and Applications*, edited by J.P. Liu et al. (Springer Science+Business Media, LLC), 2009, pp. 14-1.
2. Heczko O, Sozinov A, Ullakko K, IEEE Trans. Magn., **36**, (2000), 3266-3268.
3. K. Oikawa, L. Wulff, T. Iijima, F. Gejima, T. Ohmori, A. Fujita, K. Fukamichi, R. Kainuma, K. Ishida, *Appl. Phys. Lett.*, **79**, (2001), 3290.
4. Yu. I. Chumlyakov, I. V. Kireeva, E. Yu. Panchenko, E. E. Timofeeva, Z. V. Pobedennaya, S. V. Chusov, I. Karaman, H. Maier, E. Cesari and V. A. Kirillov, *Russ. Phys. J.,* **51**, (2008), 1016.
5. J. Kopeček, S. Sedláková-Ignácová, K. Jurek, M. Jarošová, J. Drahokoupil, P. Šittner, V. Novák: *Structure development in $Co_{38}Ni_{33}Al_{29}$ ferromagnetic shape memory alloy*, 8th th European Symposium on Martensitic Transformations, ESOMAT 2009, edited by Petr Šittner, Václav Paidar, Luděk Heller, Hanuš Seiner, 2009, article No. 02013.
6. J. Kopeček, K. Jurek, M. Jarošová, et al., *IOP Conf. Sci.: Mater. Sci. Eng.*, **7**, (2010), 012013.
7. J. Kopeček, V. Kopecký, M. Landa, O. Heczko, Mat. Sci. Forum, 738-739, 416-420, (2013)
8. B. Bártová, N. Wiese, D. Schryvers, N. J. Chapman, S. Ignácová, Acta Mater., 56 (2008), 4470-4476.
9. B. Bártová, D. Schryvers, Z. Q. Yang, S. Ignácová, P. Sittner, Scripta Mater., 57 (2007), 37- 40.
10. J.B. Lu, H. Shi, S. Sedláková-Ignácová, R. Espinoza, J. Kopeček, P. Šittner, B. Bártová, D. Schryvers, J. Alloys Comp., 572, 5-10, (2013)
11. H. Seiner, J. Kopeček, P. Sedlák, L. Bodnárová, M. Landa, P. Sedmák, O. Heczko, Acta Mater., 61, 5869-5876, (2013)
12. O. Heczko, H. Seiner, P. Sedlák, J. Kopeček, V. Kopecký, M. Landa, Eur. Phys. J. B, 86:(2), 62-1 – 62-5, (2013).

Authors would like to acknowledge the financial support from the Grant Agency of the AS CR project IAA 100100920 and Czech Science Foundation projects 101/09/0702, P107/11/0391.